Influence of the medium length on high-order harmonic generation

Delfin, C; Altucci, C; De Filippo, F; de Lisio, C; Gaarde, Mette; L'Huillier, Anne; Roos, L; Wahlström, Claes-Göran

Published in:
Journal of Physics B: Atomic, Molecular and Optical Physics

DOI:
10.1088/0953-4075/32/22/316

1999

Influence of the medium length on high-order harmonic generation

1999 J. Phys. B: At. Mol. Opt. Phys. 32 5397

(http://iopscience.iop.org/0953-4075/32/22/316)

J. Phys. B: At. Mol. Opt. Phys. **32** (1999) 5397–5409. Printed in the UK PII: S0953-4075(99)06463-9

Influence of the medium length on high-order harmonic generation

C Delfin†, C Altucci‡§, F De Filippo‡‖, C de Lisio‡‖, M B Gaarde†¶, A L'Huillier†, L Roos† and C-G Wahlström†

† Department of Physics, Lund Institute of Technology, PO Box 118, S-221 00 Lund, Sweden
‡ Istituto Nazionale di Fisica della Materia (INFM), Unitá di Napoli, Naples, Italy
§ Universitá della Basilicata, Via Anzio 10, 85100 Potenza, Italy
‖ Dipartimento di Scienze Fisiche, Universitá di Napoli 'Federico II', Complesso Universitario di Monte Sant'Angelo, Via Cintia, 80126 Naples, Italy
¶ Niels Bohr Institute, Ørsted Laboratory, Universitetsparken 5, 2100 Copenhagen, Denmark

Received 30 July 1999, in final form 6 September 1999

Abstract. We study high-order harmonic generation using a 110 fs Ti:sapphire laser loosely focused into a variable-length gas cell filled with neon or argon at 5 mbar pressure. The harmonic intensity is recorded as a function of the medium length, varying between 2 and 21 mm. Several cases are examined, the 17th and the 29th harmonic in argon, and the 29th and 51st harmonic in neon, at the same intensity 4×10^{14} W cm^{-2}. We find that the length which maximizes the harmonic yield varies from 10 mm to more than 20 mm. We discuss the different effects affecting the photon yield of the high-order harmonics.

1. Introduction

In recent years high-order harmonic generation has become a promising source of short-pulse coherent radiation in the extreme ultraviolet (XUV) range. The harmonic radiation is suitable for a number of applications, from atomic physics [1] to solid state physics [2] and plasma diagnostics [3]. A large effort has been devoted to increasing the photon number. Early studies have mostly concentrated on optimization with respect to atomic or molecular gases (see, for example, [4–9]), and to the laser wavelength [4, 10], thus addressing mostly the single-atom emission. Lompré *et al* pointed out the importance of using a loose focusing geometry [11]. Altucci *et al* studied the influence of the pressure on the harmonic yield, showing the influence of defocusing due to free electrons at high pressure [12]. Recently, several groups have studied harmonic generation using ultra-short laser pulses focused into a hollow fibre [13–15], or forming a filament [16], reporting relatively high conversion efficiencies.

The generation efficiency and the propagation of high-order harmonics in a gas medium are to a large extent controlled by phase matching, affecting both the photon yield and the coherence of the generated radiation. There are several effects contributing to phase matching:

- the *geometrical phase shift* due to focusing of the driving laser beam;
- the *phase of the single-atom dipole moment* which in the non-perturbative regime depends on the laser intensity;

0953-4075/99/225397+13$30.00

- the *dispersion* of the nonlinear medium due to the neutral atoms, as well as due to the free electrons created through *partial ionization* of the medium; and
- the *defocusing of the fundamental beam* owing to the presence of free electrons.

The harmonic yield is also affected by the *absorption* of the generated harmonics within the nonlinear medium. The first two effects are pressure independent, whereas dispersion and absorption vary linearly with the gas density. Although experimentally difficult, the most direct way to study phase matching of high-order harmonics, and possibly to observe a limitation due to absorption, is to investigate the harmonic signal as a function of the length of the nonlinear medium for a constant pressure.

In this paper we present an investigation of the harmonic yield as a function of the length of the nonlinear medium, for several harmonics of a 110 fs Ti:sapphire laser, generated in argon and neon. Our aim is not to optimize the conversion efficiency (which we do not measure), but to understand what governs phase matching in a loose focusing geometry for different test cases: harmonics in the plateau or in the cut-off regions, with or without strong ionization of the medium, and with or without significant absorption.

The laser intensity is kept constant and equal to about 4×10^{14} W cm^{-2}. The pressure in the interaction region, also fixed, is estimated to be 5 mbar. The length of the gas medium where harmonics are generated can be varied from 2 to 21 mm. We concentrate on the following four cases.

(a) The 17th harmonic in argon. This harmonic belongs to the plateau. At this wavelength, i.e. 47 nm, the absorption coefficient in argon is relatively high.
(b) The 29th harmonic in argon. This harmonic is much closer to the cut-off spectral region. The absorption is much less than for the 17th harmonic, because the photon energy corresponds to a dip in the argon absorption cross section, owing to the presence of a Cooper minimum.

In these two cases, (a) and (b), the intensity used is higher than the saturation intensity for argon, implying a high degree of ionization. In particular, the presence of free electrons should affect phase matching and more generally the propagation of the fundamental and generated fields in the nonlinear medium.

(c) The 29th harmonic in neon, belonging to the plateau.
(d) The 51st harmonic in neon, close to the plateau/cut-off transition.

In these latter two cases, the intensity is significantly weaker than the saturation intensity, so that ionization is expected to play a considerably smaller role than in argon. The absorption coefficient for both harmonics in neon is relatively small.

The paper is organized as follows. In section 2 we describe our experimental set-up. In section 3 we present our experimental results and compare them with numerical simulations using the strong-field approximation (SFA) [17] for the single-atom response. In section 4 we discuss the different contributions to phase matching, using simple one-dimensional arguments. Section 5 is devoted to a brief summary.

2. Experimental set-up

The experimental set-up is shown schematically in figure 1. The 10 Hz terawatt Ti:sapphire laser of the Lund High Power Laser Facility [18] operates at a wavelength of 800 nm and has a pulse duration of 110 fs. The 50 mm laser beam diameter is apertured down to 20 mm and then focused by a $f = 2$ m lens into a vacuum chamber. With an energy per pulse of

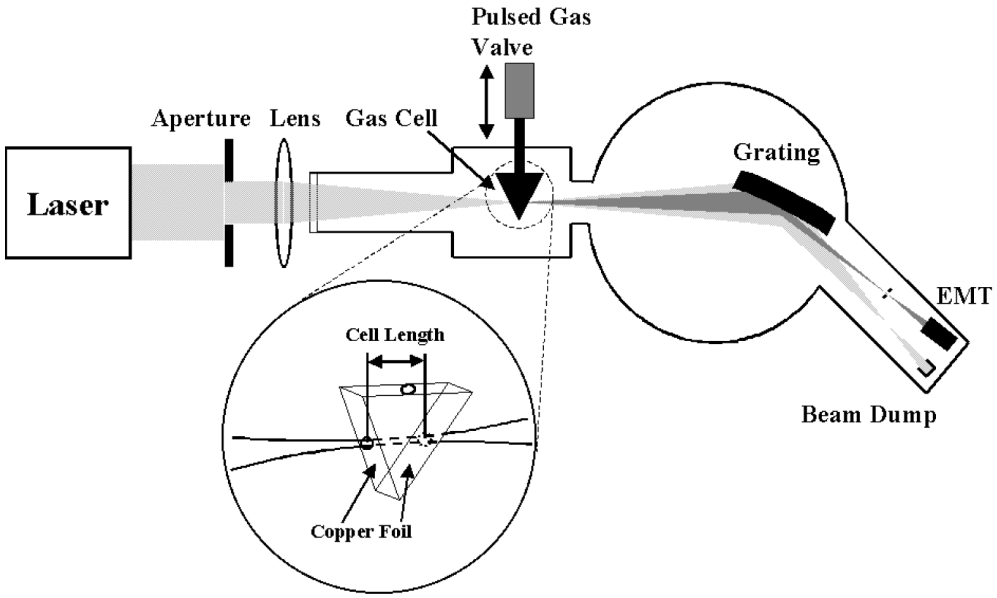

Figure 1. Experimental set-up.

approximately 9 mJ entering the chamber, the laser peak intensity I in the interaction region is estimated to be $I \approx 4 \times 10^{14}$ W cm^{-2}. Harmonics, generated in the variable length gas medium described below, are separated with a grazing-incidence toroidal grating and detected by an electron multiplier (EMT) placed behind a 200 μm exit slit. By rotating the grating a spectrum is acquired. Every point in the spectrum contains an average over 50 laser shots. To keep the intensity within an acceptable range, laser shots differing more than 15% in energy were ejected.

In order to vary the medium length while keeping the pressure constant and spatially uniform, we have designed a small windowless gas cell, which is shaped like an arrowhead (see figure 1). The gas cell lateral section is an isosceles triangle. Two versions of the gas cell are used with 32 mm height and 30 mm base and with 28 mm height and 6 mm base, respectively, the latter allowing us to investigate shorter lengths. The cell widths are chosen so that the two cells have the same volume.

In the middle of the gas cell base a 1 mm large hole is drilled where the gas is injected. A constant gas flow into the gas cell is not compatible with a good vacuum in the chamber, therefore we use a pulsed piezoelectric valve to inject the gas into the gas cell. The backing pressure of the valve is 0.5 bar and the opening time is 0.5 ms.

To minimize leakage from the gas cell, the entrance and exit holes are made as small as possible by letting the laser itself burn them in the 50 μm thin copper foil which constitutes the sides of the gas cell. The laser-drilled holes have a diameter of about 0.5 mm. We can estimate the pressure in the gas cell to be ≈ 5 mbar. This is done by consider the backing pressure, the opening time of the piezoelectric valve, the gas inlet area and neglecting leaks from the laser holes within the first few milliseconds after the valve closure time. The medium length is varied by vertically translating the gas cell perpendicularly to the laser axis. For each position the previously drilled holes are sealed, and new ones are made, so that the pressure in the gas cell is kept constant.

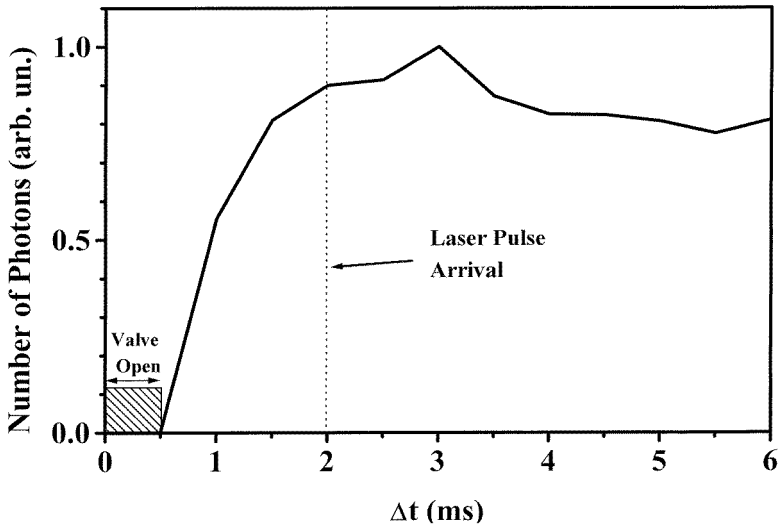

Figure 2. Harmonic photon number versus time delay, Δt, between valve opening and laser pulse arrival with $P_{\text{backing}} = 0.5$ bar and a valve opening time of 0.5 ms. The curve refers to the 23rd harmonic in neon with a medium length $L = 21$ mm.

Using in turn the two cells described above, the medium length can be varied between 2 and 21 mm. The narrow cell allows us to study medium lengths between 2 and 6 mm, and the broad one up to 21 mm. The lower limit of the medium length is set by the size of the laser-drilled holes and the dimension of the smallest cell. From isotropic expansion the decay length of the pressure outside these holes is estimated to be less than 0.5 mm.

The shortest medium length investigated is therefore 2 mm (1 mm inside the gas cell and 1 mm outside).

It is important to check that the pressure is uniform inside the gas cell, independent of the position of the laser holes, and that the same pressure is obtained for the two cells. For this purpose we monitor the harmonic yield versus the time delay between the valve opening time and the laser pulse for different positions of the gas cells, i.e. for different medium lengths. The harmonic signal increases during the first $\sim$1.5 ms, is almost constant for a couple of milliseconds and then slowly decreases. It takes more than 15 ms to empty the gas cell. Figure 2 shows, as an example, the results for the 23rd harmonic in neon for a medium length $L = 21$ mm. The pressure in the narrow gas cell reaches its stationary value slightly faster than that in the broad gas cell. In the measurements we choose the laser pulse arrival to be 1.5 and 2 ms after the valve opening time for the narrow and the broad gas cell, respectively. It is worth stressing that we find the time interval during which the harmonic signal is constant to be independent of the gas (Ar, Ne) used in the experiment and also independent of the medium length. Therefore, we consider the gas pressure inside the gas cells to be spatially uniform during the propagation of the laser pulse and to rule out undesired effects due to spatial gas density gradients inside the gas cells. In addition, we find that the harmonic signal is independent of the gas cell used as long as the medium length is the same. (The two gas cells are filled to the same pressure.)

3. Experimental results and three-dimensional numerical simulations

The experimental results for cases (a)–(d) mentioned in the introduction are presented as full squares in figure 3(*a*)–(*d*). The number of photons for each harmonic, obtained by integrating its spectrum, is reported as a function of the medium length. The number of photons increases first rather rapidly, depending on the harmonic order and the gas medium, and then saturates. For all the investigated harmonics the number of photons increases with increasing length up to 10–15 mm. For the 17th harmonic in argon the signal slowly starts to decrease for lengths longer than 11 mm, probably due to absorption which is important for this

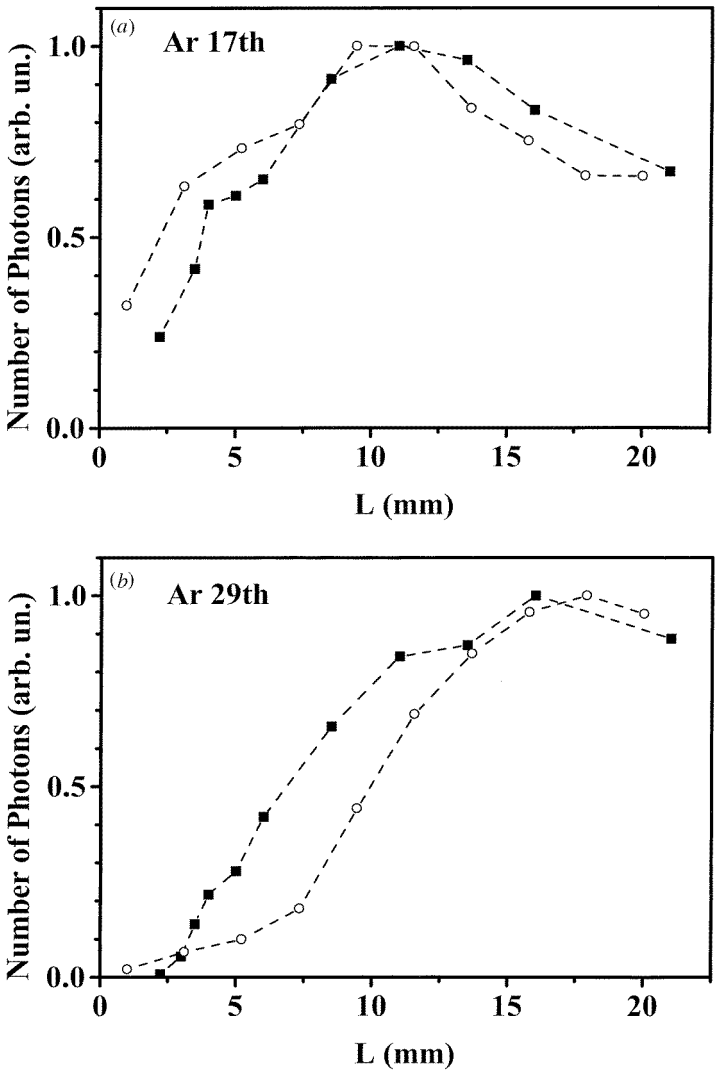

Figure 3. Harmonic intensity versus medium length, L, for the (*a*) 17th harmonic in argon; (*b*) 29th harmonic in argon; (*c*) 29th harmonic in neon and (*d*) 51st harmonic in neon at a laser intensity $I = 4 \times 10^{14}$ W cm^{-2} and a gas pressure of 5 mbar. Experimental result are indicated by full squares and theoretical simulations by open circles.

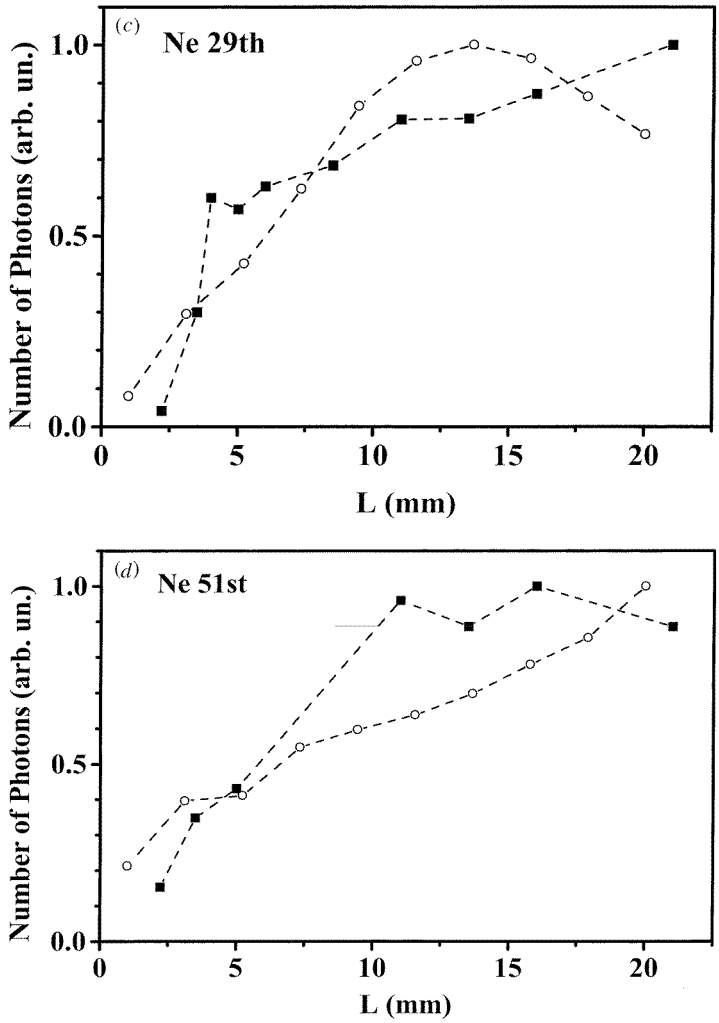

Figure 3. Continued.

harmonic, while for the other harmonics it continues to increase slowly or stays approximately constant.

In order to explain the experimental results we performed a series of numerical calculations. Our method is described extensively elsewhere [19]. First, we calculate the single-atom dipole moment $d_q(I)$ for a given harmonic q as a function of the intensity I of the driving field, using the strong-field approximation [17]. Secondly, we propagate the harmonic field through the macroscopic gas medium, by solving the wave equation in the paraxial and slowly varying envelope approximations. We use the calculated single-atom dipole moments as an input to the nonlinear part of the polarization field:

$$P_q^{\mathrm{NL}}(r, z, t) = 2\mathcal{N}_{\mathrm{a}}(r, z, t)\, d_q(I(r, z, t)) \exp(\mathrm{i}q\phi_1(r, z, t))$$

using cylindrical coordinates. In the above equation, $\mathcal{N}_{\mathrm{a}}$ is the space and time-dependent atomic density, $\phi_1(r, z, t)$ the phase of the fundamental which can vary in time if the refractive

index at the fundamental frequency is time dependent. The variation in time of the atomic density due to ionization introduces several effects, one of course being the depletion of the nonlinear medium which reduces the signal. The presence of the free electrons resulting from ionization in turn introduces a time- and space-dependent variation of the refractive index in the gas (dispersion due to free electrons). The temporal variation of the refractive index induces a broadening and a blueshift of the fundamental bandwidth, whereas the spatial variation induces a defocusing of the laser beam. We take all of these effects into account in our calculations. In addition, we consider absorption as well as the effect of dispersion due to neutral atoms.

The phase advance of the truncated Gaussian beam used in the experiment (beam diameter 5 cm, aperture 2 cm), is calculated numerically by performing a Hankel transform of the electric field after the aperture. The phase variation is not as rapid across the focus as the phase variation of a Gaussian beam with a diameter equal to that of the aperture. In our experimental conditions the phase advance is only about half as rapid as that of a Gaussian beam with diameter 2 cm. The intensity of a truncated Gaussian beam also varies more slowly across the focus than that of a Gaussian beam with the same diameter as the aperture. In our three-dimensional numerical simulation the laser beam is modelled as a Gaussian, with a confocal parameter of 5 cm, so as to approximate well both the beam intensity and the phase variation close to the focus.

All the parameters used in the calculations are set to mimic the experimental conditions. The peak intensity is set to 4×10^{14} W cm^{-2}, the pressure in the gas jet to 5 mbar, the atomic density is taken to have a square distribution along the propagation axis and the length of the medium is varied between 1 and 20 mm.

The results of the numerical simulations are plotted as open circles together with the experimental result in figures 3(*a*)–(*d*). They have been scaled to the same maximum signal as in the experiments. The simulations show a similar trend to the experiment: all the results first show an increase with the medium length, then a saturation, followed by a slow decrease (except for the 51st harmonic in neon).

In the calculation, one can conveniently study the different contributions to the phase-matching process. In figure 4 we show calculated results for the 29th harmonic in argon where we have 'switched off' different effects in turn. With full circles we show the full result, and as full squares the result when omitting the dipole phase. The curve with open squares shows the result of neglecting the effect of defocusing (but including the dipole phase). The result shown with full diamonds results from excluding all effects due to ionization. The open circles refer to results obtained by neglecting ionization and absorption. For this harmonic two effects significantly influence phase matching. First, the dipole phase really helps to achieve good phase matching as seen by the large decrease when this phase contribution is omitted. The presence of the dipole phase increases the coherence length compared to without it. Secondly, ionization, and especially depletion of the neutral medium due to the high laser intensity plays an important role and reduces the harmonic yield.

By performing this type of analysis for all of the harmonics, we can estimate what are the important factors in each case. For both the harmonics in neon we find as for the 29th harmonic in argon, that the dipole phase helps to achieve good phase matching. In fact, when we exclude the contribution from the dipole phase, the number of photons remains very small and is essentially independent of the length of the medium, apart from small oscillations. For the 29th harmonic in neon, ionization plays very little role. At the longest medium lengths the dispersion from free electrons and the resulting defocusing even slightly increases the photon yield (by 25%) compared to without it. The decrease in the number of photons observed from about 13 mm is caused by absorption. In the absence of absorption, the curve would saturate at this length. For the 51st harmonic in neon, absorption is not important. Depletion of the

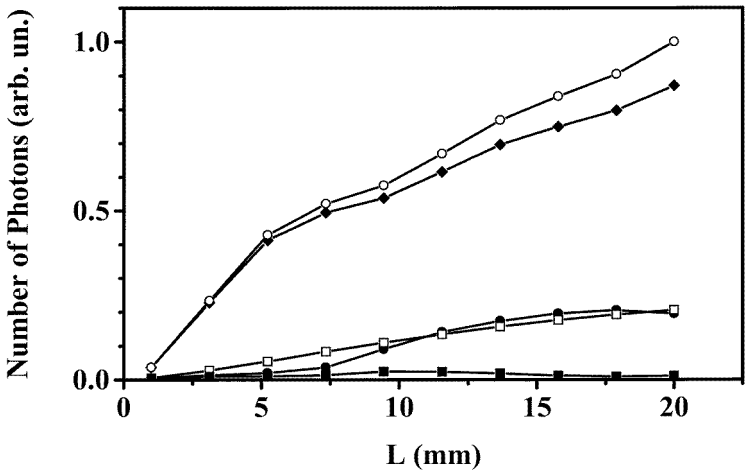

Figure 4. Theoretical results for the 29th harmonic in argon. Full circles represent the full result and full squares the result when omitting the dipole phase. The curve with open squares illustrates the result when omitting the effect of defocusing (but including the dipole phase). The result shown with full diamonds results from excluding all effects due to ionization. Open circles represent the results when ionization and absorption have been neglected.

neutral medium due to ionization in general decreases the photon yield by approximately a factor of two, whereas dispersion from free electrons only plays a role at the longest medium lengths, where it causes a reduction of the order of 30%.

The 17th harmonic in argon is different from the other harmonics in several aspects. First, the contribution of the dipole phase is *not* very important for the number of photons achieved. And secondly, absorption is by far the dominant effect, reducing the number of photons by more than an order of magnitude at the longest length. The different effects due to ionization also contribute to reduce the photon yield.

Thus, we find that for most of the investigated harmonics, the dipole phase is important for achieving good phase-matching conditions, though not for the 17th harmonic in argon. We also find that at these low pressures, the ionization-induced defocusing plays a marginal role. To investigate in more detail the interplay between the different phase contributions, and thus to interpret the experimental and numerical results, we present in the following a simple one-dimensional on-axis model of phase matching. This will allow us to obtain a better intuitive understanding of phase matching of the high-order harmonics.

4. One-dimensional model of phase matching

We discuss, in turn, the different contributions to the phase mismatch between the polarization of the nonlinear medium due to the intense laser field and the harmonic field which is generated.

First, we define a local coherence length as

$$L(z) = \pi \Big/ \frac{\mathrm{d}\delta\phi(z)}{\mathrm{d}z}.$$

$L(z)$ can be positive or negative, the sign indicating the sense of variation of the phase. We then show how the different contributions can add to give good phase matching.

4.1. Geometrical phase

The on-axis phase advance of a Gaussian beam across the focus reads $\phi_1(z) = \tan^{-1}(2z/b)$, where b is the laser confocal parameter. The phase difference between the polarization of the qth harmonic and the generated harmonic field on-axis, induced by focusing is then

$$\delta\phi_{\text{geo}}(z) = \phi_q(z) - q\phi_1(z)$$

where $\phi_q(z)$ is the on-axis phase advance of the generated harmonic field. In general, the divergence of the harmonic field is smaller than, or comparable to, the divergence of the fundamental field [20] so that $\phi_q(z) \lesssim \phi_1(z)$. For high harmonic orders, this leads to $\delta\phi_{\text{geo}}(z) \approx -q\phi_1(z)$.

The phase variation for the truncated Gaussian, used in the experiment is obtained through a numerical calculation, and leads to $L_{\text{geo}}(z) \approx -65/q$ mm. In table 1, we give L_{geo} for the 17th (a), 29th (b, c) and 51st (d) harmonics.

Table 1. Calculated coherence length (mm) for the geometrical phase dispersion due to neutral atoms and dispersion due to free electrons. The absorption decay length (mm) is also given.

	17th Ar (a)	29th Ar (b)	29th Ne (c)	51st Ne (d)
L_{geo}	−3.8	−2.2	−2.2	−1.3
L_{disp}	−23	−17	−40	−22
L_{e}	1.3	0.8	13	7.3
L_{abs}	2.4	72	10	13

4.2. Dispersion due to neutral atoms

The phase difference induced by dispersion in the neutral medium is

$$\delta\phi_{\text{disp}}(z) = (k_q - qk_1)z$$

where k_q and k_1 are the wavevectors at frequency $q\omega$ and ω, respectively. $\Delta k = k_q - qk_1 = (2\pi q\omega/c)\mathcal{N}(\alpha_{\text{pol}}(q\omega) - \alpha_{\text{pol}}(\omega))$, where $\mathcal{N}$ is the density of neutral atoms. The dynamic polarizability $\alpha_{\text{pol}}(\omega)$ is positive at 800 nm, equal to about 1.6×10^{-24} cm^3 for argon and 0.4×10^{-24} cm^3 for neon [21]. Since the photon energy for the harmonics considered in the present work is above the ionization limit, $\alpha_{\text{pol}}(q\omega)$ is negative but of the same order of magnitude as $\alpha_{\text{pol}}(\omega)$ [22]. We estimate the number of neutral atoms in the following way. The intensity-dependent ionization rates have been calculated by applying a tunnelling ionization formula [23]. By solving the propagation equation for the fundamental field through the partially ionized medium, we can estimate the amount of ionization in the medium at the peak of the harmonic pulse. For medium lengths of 10 mm we get approximately 50% ionization in the case of argon and 3% in the case of neon. Note that in argon, where the intensity is above saturation, defocusing leads to a decrease in the intensity and thereby a reduction of the depletion. We assume here for the sake of simplicity that the ionization yield is constant over the examined region. In reality it increases and then decreases along the propagation axis, depending on the laser intensity, but only by a few per cent over the medium length. The coherence lengths due to the linear dispersion L_{disp}, at a pressure of 5 mbar, corresponding to the four cases are given in table 1.

4.3. Dispersion due to free electrons

In general, free electrons generated in the nonlinear medium lead to deterioration of phase matching. The phase mismatch induced by the free electrons is $\delta\phi_e \approx z\omega_p^2 q/2c\omega$, where ω_p is the plasma frequency. In table 1 we give the coherence length L_e, accounting for the effect of the free electrons. The ionization yields used are the same as above.

4.4. Dipole phase variation

The laser-induced polarization has an intrinsic intensity-dependent phase, which is that of the single-atom dipole moment, arising from the phase of the electronic wavefunction [24]. In order to better understand the origin of this intensity-dependent phase let us briefly recall the implications of the semiclassical model for harmonic generation.

The semiclassical model assumes that an atom interacting with an intense laser field can be described as having only one active electron. The electron experiences the sum of the atomic core static electric field and the oscillating intense electromagnetic laser field. It can tunnel through the barrier formed by the resulting potential and subsequently be accelerated by the laser field and driven back towards the core and recombine. When decaying to the ground state, it gives rise to the emission of a high-energy photon. For the generation of some specific harmonic, there are several possible *trajectories* such that the electron returns to the core with the correct energy, depending on the times of release from and return to the core. Each of these trajectories contributes to the dipole moment with a phase which is proportional to the intensity of the driving field. The proportionality factor, or *phase coefficient* α, is closely related to the amount of time the electron spends in the continuum [24]. For each trajectory (labelled by j) this leads to an intensity-dependent variation of the phase:

$$\delta\phi_{\mathrm{dip},j}(z) = -\alpha_j I(z)$$

where $I(z)$ denotes the intensity of the fundamental field. The phase coefficients can be determined theoretically, using the semiclassical model [24] and the quantum path analysis described in [25]. Within this model, the dominant contribution to the dipole moment is that of the second trajectory, with phase coefficient α_2, for all of the harmonics investigated this corresponds to a return of the electron after approximately one laser period. We calculate α_2 to be between 20 and 28 $\times 10^{-14}$ cm^2 W^{-1} for the different cases studied. To estimate the effective coherence length due to the dipole phase, we need to know the variation of the laser intensity in the medium. The variation of the intensity for the truncated Gaussian beam used in the experiment is calculated numerically. In figure 5(*a*), we plot for the 29th harmonic in neon as a broken line the numerically calculated local coherence length corresponding to the contribution of the second trajectory (α_2). $|L_{\mathrm{dip}}(z)|$ is maximum at focus, where $\mathrm{d}\delta\phi(z)/\mathrm{d}z = 0$. $L_{\mathrm{dip}}(z)$ is negative before and positive after the focus.

4.5. Total coherence length

To conclude this analysis, let us now consider the total local coherence length on axis. We sum the phases from all contributions, giving

$$L_{\mathrm{tot}} = \left[L_{\mathrm{geo}}^{-1} + L_{\mathrm{dip}}^{-1} + L_{\mathrm{disp}}^{-1} + L_{\mathrm{e}}^{-1}\right]^{-1}$$

which is represented as a full curve in figure 5(*a*) for the 29th harmonic in neon. In that figure we also plot as a dotted line the coherence length obtained by excluding the contribution from the dipole phase.

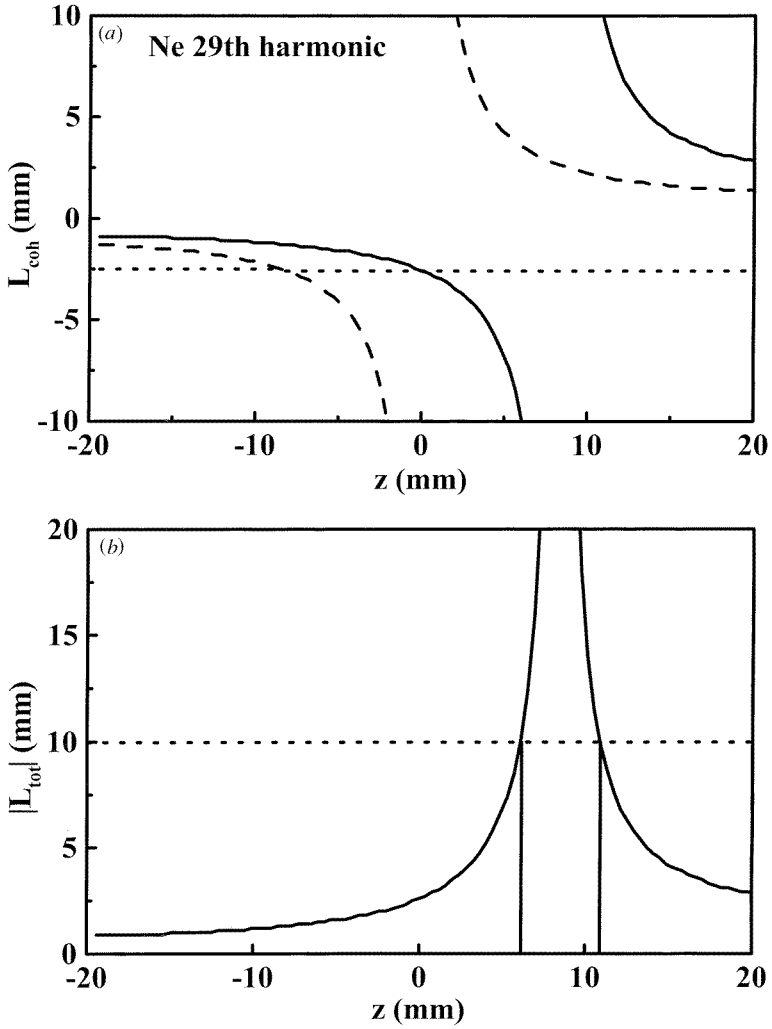

Figure 5. Calculated coherence lengths for the 29th harmonic in neon with a 1D model. (*a*) Total coherence length (full curve), coherence length coming from the dipole phase excluded (dotted curve) and coherence length from the dipole phase (broken). The absolute value of the total coherence length is shown in (*b*). The vertical lines indicate the region where $|L_{\rm coh}|$ is longer than 10 mm.

Among the different coherence lengths considered, the coherence length due to the dipole phase has the peculiarity that it varies significantly close to the focus (and changes sign). The other contributions are approximately constant. There is a region on-axis where the dipole phase significantly helps to achieve phase matching (where the total coherence length becomes very long). This region is before or after the focus depending on the sign of the effective coherence length due to all the other effects, except the dipole phase. The loose focusing geometry ensures that this region is relatively long. In agreement with the full simulation of section 3, the variation of the dipole phase across the focus results in good phase matching with a coherence length which is larger than 10 mm over a length at least 5 mm as shown in figure 5(*b*).

The 'anomaly' presented by the 17th harmonic in Ar, where the dipole phase does not help in achieving good matching is not reproduced by our simple one-dimensional (1D) analysis. It might be due to more complicated single-atom dynamics involving contributions of several trajectories (with different phase coefficient) and/or to three-dimensional effects.

4.6. Absorption

Finally, it is important to also consider the influence of absorption of the generated harmonics in the nonlinear medium. The absorption coefficient at frequency $q\omega$ is related to the one-photon ionization cross section σ_q by $\kappa_q = \mathcal{N}\sigma_q$. The absorption length, over which the intensity of the generated field has decreased by a factor of e^{-1} is $L_{\text{abs}} = 1/\kappa_q$. The absorption cross sections for the four cases studied are: (a) 33, (b) 1.1, (c) 7.7 and (d) 6.2 Mbarn. The corresponding absorption lengths at a pressure of 5 mbar are given in table 1. Apart from the 17th harmonic in argon these lengths are relatively long, and the harmonic emission is not dominated by absorption at the low pressure used in the experiment, in good agreement with the numerical results in section 3.

5. Summary

We show that with loose focusing and low densities, the optimum length of the nonlinear medium is rather long, 10–20 mm, much longer than what is normally used in pulsed gas jets for harmonic generation. This is also much longer than expected when considering only geometrical phase shift and dispersion. Our interpretation, supported by 1D and 3D calculations, is that the dipole phase in general helps to achieve good phase-matching conditions. We also show that it can be advantageous to truncate the laser beam, to obtain a 'top hat' distribution before the focusing lens, in order to have a slow variation of the intensity and the phase along the propagation axis in the interaction region.

Acknowledgments

We acknowledge the support of the Swedish Natural Science Research Council and the EC 'Access to Large Scale Facilities' Programme (contract no ERBFMGECT950020).

References

[1] Gisselbrecht M, Descamps D, Lyngå C, L'Huillier A, Wahlström C-G and Meyer M 1999 *Phys. Rev. Lett.* **82** 4607
[2] Haight R and Peale D R 1993 *Phys. Rev. Lett.* **70** 3979
[3] Theobald W, Hässner R, Wülker C and Sauerbrey R 1996 *Phys. Rev. Lett.* **77** 298
[4] Balcou Ph and L'Huillier A 1993 *Phys. Rev.* A **47** 1447
[5] Kondo K, Tamida T, Nabekawa Y and Watanabe S 1994 *Phys. Rev.* A **49** 3881
[6] Wahlström C-G, Borgström S, Larsson J and Pettersson S-G 1995 *Phys. Rev.* A **51** 585
[7] Fraser J D, Hutchinson M H R, Marangos J P, Shao Y L, Tisch J W G and Castillejo M 1995 *J. Phys. B: At. Mol. Opt. Phys.* **28** L739
[8] Lyngå C, L'Huillier A and Wahlström C-G 1996 *J. Phys. B: At. Mol. Opt. Phys.* **29** 3293
[9] Donnelly T, Ditmire T, Neuman K, Perry M D and Falcone R W 1997 *Phys. Rev. Lett.* **76** 2472
[10] Ditmire T, Crane J K, Nguyen H, DaSilva L B and Perry M D 1995 *Phys. Rev.* A **51** R902
[11] Lompré L-A, L'Huillier A, Monot P, Ferray M, Mainfray G and Manus C 1990 *J. Opt. Soc. Am.* B **7** 754
[12] Altucci C, Starczewski T, Mével E, Wahlström C-G, Carré B and L'Huillier A 1996 *J. Opt. Soc. Am.* B **13** 148
[13] Schnürer M, Cheng Z, Sartania S, Hentschel M, Tempea G, Brabec T and Krausz F 1998 *Appl. Phys.* B **67** 263

[14] Rundquist A, Durfee C G III, Chang Z, Herne C, Backus S, Murnane M M and Kapteyn H C 1998 *Science* **280** 1412
[15] Constant E, Garzella D, Breger P, Mével E, Dorrer Ch, Le Blanc C, Salin F and Agostini P 1999 *Phys. Rev. Lett.* **82** 1668
[16] Tamaki Y, Itatani J, Nagata Y, Obara M and Midorikawa K 1999 *Phys. Rev. Lett.* **82** 1422
[17] Lewenstein M, Balcou Ph, Ivanov M Yu, L'Huillier A and Corkum P 1994 *Phys. Rev.* A **49** 2117
[18] Svanberg S, Larsson J, Persson A and Wahlström C-G 1994 *Phys. Scr.* **49** 187
[19] L'Huillier A, Balcou Ph, Candel S, Schafer K J and Kulander K C 1992 *Phys. Rev.* A **46** 2778
[20] Saliéres P, Ditmire T, Perry M D, L'Huillier A and Lewenstein M 1996 *J. Phys. B: At. Mol. Opt. Phys.* **29** 4771
[21] Leonard P J 1974 *At. Data Nucl. Data Tables* **14** 21
[22] L'Huillier A, Li X F and Lompré L-A 1990 *J. Opt. Soc. Am.* B **7** 527
[23] Ilkov F A, Decker J E and Chin S L 1992 *J. Phys. B: At. Mol. Opt. Phys.* **25** 4005
[24] Lewenstein M, Saliéres P and L'Huillier A 1995 *Phys. Rev.* A **52** 4747
[25] Balcou Ph, Dederichs A S, Gaarde M B and L'Huillier A 1999 *J. Phys. B: At. Mol. Opt. Phys.* **32** 2973